Thermochimica Acta 520 (2011) 80–83

Contents lists available at ScienceDirect

Thermochimica Acta

journal homepage: www.elsevier.com/locate/tca

Phase equilibria in the $PbSb_2Te_4$–InSb system

V. Vassilev*, D. Atanassova, I. Mihaylova, V. Parvanova, L. Aljihmani

University of Chemical Technology and Metallurgy, 8 Kliment Ohridski Blvd., 1756 Sofia, Bulgaria

ARTICLE INFO

Article history:
Received 15 November 2010
Received in revised form 14 March 2011
Accepted 25 March 2011
Available online 5 April 2011

Keywords:
Chalcogenides
Semiconductors
Differential thermal analysis
X-ray diffraction
Phase equilibria

ABSTRACT

A phase diagram of the $PbSb_2Te_4$–InSb system, which is polythermal cross section of the three-component PbTe–Sb_2Te_3–InSb system, was built using DTA, XRD, microhardness and density measurements. The system contains the $PbSb_2Te_4{\cdot}(2\pm\delta)$InSb compound of variable composition, incongruently melting at $530\pm5\,^{\circ}C$, and with asymmetric area of homogeneity shifted to the side rich in InSb ($+\delta = 0$–2). The $PbSb_2Te_4{\cdot}2$InSb compound crystallizes in orthorhombic symmetry with unit cell parameters: $a = 7.7640$ Å; $b = 6.4144$ Å; and $c = 3.6010$ Å, $\alpha=\beta=\gamma=90^{\circ}$. The system also contains $PbSb_2Te_4$ and InSb based boundary solid solutions extended from 0 to 10 and from 95 to 100 mol% InSb, respectively, at room temperature.

1. Introduction

The binary $PbSb_2Te_4$–InSb system was studied neither in respect of the phase equilibria therein, nor in respect of the possibility of formation of intermediate phases with new properties or formation of boundary solid solutions. The initial components of this system are typical narrow-bandgap semiconductors.

The phase diagram of the Sb_2Te_3–PbTe system was plotted for the first time by Abrikosov et al. [1], then supplemented by Hirai et al. [2], Reynolds [3], and finally specified by Shelimova et al. [4]. The system is of eutectic type, and, according to recent data, contains two intermediate compounds with compositions $PbSb_2Te_4$ and $PbSb_4Te_7$, respectively, proven by XRD [4]. The $PbSb_2Te_4$ compound is formed by a peritectic reaction at 587 °C for 300 h; it has a layered structure similar to the tetradymite one, with unit cell parameters $a = 0.4351$, and $c = 4.1712$ nm [4].

The $PbSb_2Te_4$ compound is new thermoelectric material of p-type conductivity and energy gap of $\Delta E_o = 0.27$ eV at 0 K [5–7].

The phase diagram of the In–Sb system is of eutectic type with degenerated eutectics on the In side [8]. It is characterized by the formation of one compound InSb, which melts congruently at 530 °C [8]. The compound InSb crystallizes in a sphalerite-type lattice with unit cell parameter $a = 0.6478$ nm [9,10].

The energy gap value ΔE_o of InSb is 0.23 eV [11] at 0 K which is retained to 77 K, and above this temperature linearly decreases to 0.17 eV at 300 K [11].

The above data on the structure and thermoelectrical properties of the $PbSb_2Te_4$–InSb system initial components suggests:

(a) The existence of at least one intermediate compound and the formation of boundary solid solutions.
(b) The production of new $PbSb_2Te_4$ based materials with good thermoelectric properties (coefficient of thermoelectric efficiency $z = \alpha^2\sigma/\lambda \geq 3\times10^{-4}\,K^{-1}$).

The proven thermoelectric properties of $PbSb_2Te_4$ and the high values of σ and α for InSb unequivocally support this assumption.

In this sense, the purpose of this work is to study the phase equilibria in the polythermal cross section $PbSb_2Te_4$–InSb of the three-component PbTe–Sb_2Te_3–InSb system, using the classical methods (differential thermal analysis (DTA), X-ray diffraction analysis (XRD), and microhardness and density measurements) and to determine the solid solution boundaries and intermediate phase compositions (if any) with a view to the further complex study of their properties.

2. Experimental

The $(PbSb_2Te_4)_{100-x}(InSb)_x$ system was studied using 17 compositions in the concentration range of $0 \leq x \leq 100$ mol% InSb produced via direct single temperature synthesis by mixing $PbSb_2Te_4$ and InSb in proper proportions in vacuum (to residual pressure of 0.133 Pa) and sealed under vacuum quartz ampoules. The initial components, $PbSb_2Te_4$ and InSb, were synthesized from elements of 4 N (Pb, Sb) and 5 N (In, Te) purity using the same method. The maximum temperature of synthesis (T_{max}) was within

* Corresponding author. Tel.: +359 2 8163388.
E-mail address: venciv@uctm.edu (V. Vassilev).

0040-6031/$ – see front matter © 2011 Published by Elsevier B.V.
doi:10.1016/j.tca.2011.03.019

the range of 650–900 °C and was defined by the composition of samples. The ampoules were heated at rate of 10 °C min^{-1} until the maximum temperature of synthesis was reached, as the system was tempered for 2 h at 500 and 800 °C. In the final synthesis phase of the samples falling within the concentration range from 0 to 60 mol% InSb a vibration stirring of the melt was performed at T = T_{max} for 2 h, cooling to 150 ± 5 °C, and tempering at this temperature for 5 h. The samples outside this concentration range were synthesized under the same conditions, except for the tempering at 150 °C which continued for 120 h. On completion of the final thermal treatment all samples were cooled in turned off furnace.

The phase transformations of the samples were studied by DTA (device of the system F. Paulik–J. Paulik–L. Erdey by the MOM-Hungary company, Stepanov quartz vessels vacuumed and sealed under residual pressure of ~0.1 × 10^{-2} Pa, reference substance – calcinated γ-Al_2O_3, heating rate of 10 °C min^{-1}, amount of the studied and reference substance – 0.3 g), and XRD (TUR-M61 device, using CuK_α radiation and Ni-filter, θ = 5–40°). The Vickers microhardness was measured using a PMT-3 microhardness tester and a MIM-7 microscope at a load of 10 g and 20 g, and the density was measured by a hydrostatic method using toluene as a reference liquid.

The new phase was indexed by the Ito's method for indexing of XRD patterns of powders [12]. It does not depend on the symmetry of the crystal and is based on the fact that each reflex on the pattern corresponds to a vector in the reverse lattice space. The choice of three vectors, which lie on different planes, determines the edges of the elementary cell and the choice of three more vectors determines the angles between the axes. This corresponds to a choice of six appropriate lines from the roentgenogram of the powder. If a proper elementary cell is chosen, the method allows the indexing of all lines from the XRD pattern. This method is very fast and suitable for indexing of systems with low symmetry (monoclinic or triclinic).

3. Results and discussions

The synthesized InSb and $PbSb_2Te_4$ were subjected to XRD investigations. The diffraction lines of the synthesized materials coincide with the published data [4,9,10].

The XRD analysis results of the samples from the $PbSb_2Te_4$–InSb system are summarized in a schematic diagram of the X-ray diffraction lines (Fig. 1).

New diffraction lines were observed within the concentration range from 50 to 80 mol% InSb different from the $PbSb_2Te_4$ and InSb patterns. Within the concentration ranges from 0 to 10, and from 95 to 100 mol% InSb, the diffraction patterns are smoothly shifted towards one and the same direction.

The phase transformation temperatures of the studied samples were determined by the heating curves (Table 1).

The thermal effects within the concentration range from 0 to 60 mol% InSb, corresponding to the complete melting of the samples, are relatively weak. This is most probably related to the incongruent melting of the initial $PbSb_2Te_4$ compound [4] as a result of which it decomposes to PbTe + L (liquid). Therefore, the samples falling within this concentration interval were subjected to thermal annealing at T = 150 ± 5 °C for 120 h.

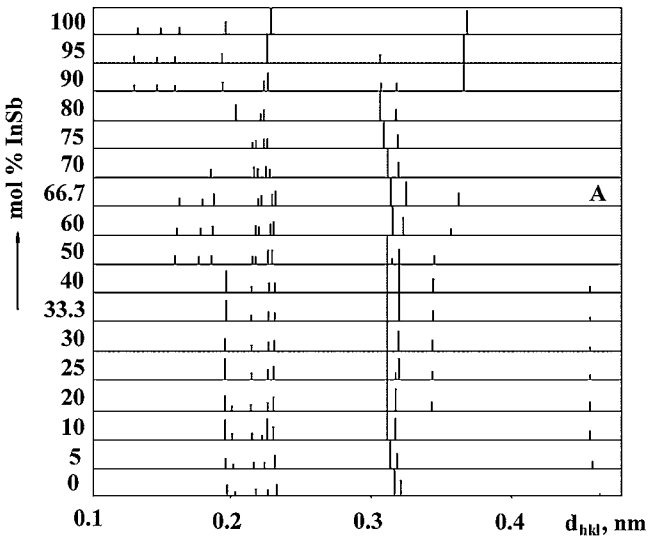

Fig. 1. Schematic diagram of the X-ray diffraction lines for the $PbSb_2Te_4$–InSb system.

All recorded effects of the thermograms are endothermic. The most clearly expressed effects (high peak and large area) are these in columns 4, 2, and 3 (the temperatures of endothermal effects in column 4 depend on the composition of the samples, while the phase transition temperatures in columns 2 and 3 are temperature independent). The thermoeffects in column 5 correspond to the temperature of complete melting of the samples and some of these temperatures outline the liquidus line of the $PbSb_2Te_4$–InSb system. Concentration areas with registered thermal effects, which do not depend on the composition, exist: 500 ± 5 °C ($10 \le x \le 40$), 530 ± 5 °C ($50 \le x \le 80$) and 460 ± 5 °C ($80 \le x \le 95$), in columns 2, 3, and 4, respectively. A similar dependence is characteristic of the non-variant equilibria or phase transitions of the $\alpha \leftrightarrow \beta$ type.

Due to the similar physicochemical properties of $PbSb_2Te_4$, InSb, and the intermediate compound on the one hand and the incongruent melting of $PbSb_2Te_4$ on the other, it is difficult to investigate the microstructure of the samples which in its turn reflects on the measurement of the microhardness (HV). In order to determine the HV, the polygons of the most probable distribution of this property are plotted. The number of phases in a sample, i.e. one phase (a single-phase sample), two phases (a two-phase sample), etc., can be judged by the characteristic type of these polygons (number of maximums). The initial components ($PbSb_2Te_4$ and InSb) and the samples, which composition falls within the concentration range

Table 1
Temperatures of endothermal effects of samples from the $PbSb_2Te_4$–InSb system.

Composition (mol%)		Temperature (°C)					Composition (mol%)		Temperature, (°C)				
$PbSb_2Te_4$	InSb	1	2	3	4	5	$PbSb_2Te_4$	InSb	1	2	3	4	5
100	0				575	637	50	50		525			525
95	5				560	620	40	60		530			557
90	10	435	500			595	33.3	66.7		530			567
80	20		495		530	560	30	70	445	535			570
75	25		500			550	25	75	310	528			580
70	30				515	?	20	80		525	460		565
66.7	33.3		495		510	540	10	90			460		460
60	40		500			520	5	95			460		500
							0	100					535

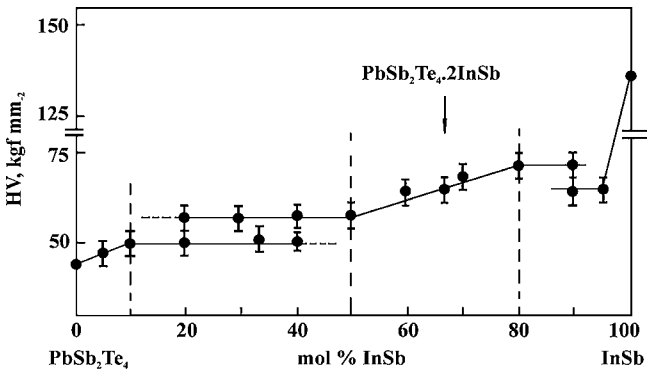

Fig. 2. Dependence of microhardness on the sample composition of the $PbSb_2Te_4$–InSb system.

from 50 to 80 mol% InSb, are single-phase and the others are two-phase (the sample phase refers to room temperature).

The microhardness of the studied samples is within the range of 45–142 kgf mm^{-2} and the microhardnesses of the initial components – $HV_{PbSb_2Te_4} = 45$ kgf mm^{-2} and $HV_{InSb} = 138$ kgf mm^{-2}. The property–composition diagram, i.e. the HV(x) dependence, is shown in Fig. 2.

The values obtained for the density d of the samples in the $PbSb_2Te_4$–InSb system fall between the values of the densities corresponding to the initial components, $PbSb_2Te_4$ and InSb: $d_{PbSb_2Te_4} = 7.50$ g cm^{-3} and $d_{InSb} = 5.78$ g cm^{-3}. The $d(x)$ diagram of the studied system samples is shown in Fig. 3.

The simultaneous comparison of the DTA and XRD results with the results from the HV and d measurements gave us the reason to outline the following features of the $(PbSb_2Te_4)_{1-x}(InSb)_x$ system: the presence of $PbSb_2Te_4$ and InSb base bounded solid solutions, on the one hand, and on the other, the existence of intermediate compound with a large area of homogeneity.

(a) The shift of the diffraction patterns (Fig. 1) and the typical HV(x) and $d(x)$ variation (Figs. 2 and 3) within the concentration ranges of $0 \le x \le 10$ and $95 \le x \le 100$ mol% InSb are unequivocally related to the presence of bounded solid solutions based on the initial components.

(b) The temperature of endoeffects at 530 ± 5 °C does not depend on the composition of the studied samples (Table 1). However, their area depends on the sample composition and the maximum area was at x = 66.7 mol% InSb. The area under the thermal effects decreases to the left and to the right of this point (Tamman triangle method), i.e. at this point an intermediate compound exists with most probable composition of $PbSb_2Te_4{\cdot}2InSb$. This is a direct evidence for the existence of an intermediate phase in support of these assumptions. The dependence observed between the area under the thermal effects and the composition excludes the assumption of a phase transition of the $\alpha \leftrightarrow \beta$ type.

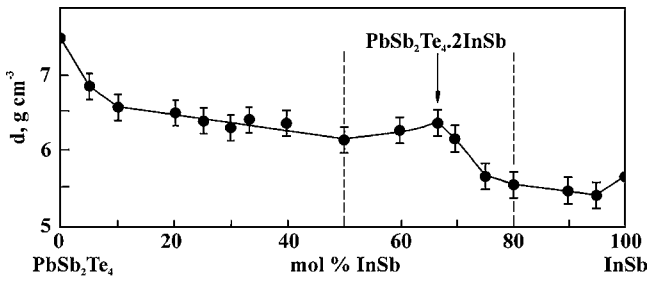

Fig. 3. Dependence of density and sample composition of the $PbSb_2Te_4$–InSb system.

Table 2
X-ray diffraction data from indexing of the $PbSb_2Te_4{\cdot}2InSb$ compound.

N	θ (°)	d_{exp} (Å)	I (%)	hkl	d_c (Å)
1.	5.68	7.7825	8	1 0 0	7.7640
2.	6.90	6.4114	7	0 1 0	6.4144
3.	11.65	3.8144	14	2 0 0	3.8820
4.	12.35	3.6013	71	0 0 1	3.6010
5.	13.70	3.2522	89	1 0 1, $\bar{1}$ 0 1	3.2667
6.	14.20	3.1400	100	0 1 1, 0 1 $\bar{1}$	3.1400
7.	19.70	2.2850	47	1 2 1, 1 2 $\bar{1}$	2.2886
8.	19.85	2.2684	30	?	?
9.	20.60	2.1892	41	0 3 0	2.1381
10.	20.88	2.1611	26	3 0 1, 3 0 $\bar{1}$	2.1016
11.	24.52	1.8560	32	4 1 0, 4 $\bar{1}$ 0	1.8578
12.	25.80	1.7697	12	$\bar{3}$ 2 1, 3 2 1	1.7578
13.	29.55	1.5618	7	0 2 2, 0$\bar{2}$2	1.5700

On the other hand, within the concentration range of $50 \le x \le 80$ mol% InSb new diffraction patterns appear, different from the $PbSb_2Te_4$ and InSb ones, with maximum intensity and "purity" of the peaks for the composition containing 66.7 mol% InSb, i.e. at this composition an intermediate compound exists. The diffraction patterns of the intermediate compound are shifted within the same range (Fig. 1) towards decrease of the cleavage spacing d_{hkl}, i.e. it has variable composition and should be recorded as $PbSb_2Te_4$ $(2 \pm \delta)$InSb, wherein: $-\delta = 0$–1; $+\delta = 0$–2.

The linear course of the HV(x) dependencies of the three compounds within the concentration ranges $0 \le x \le 5$, $50 \le x \le 80$, and $95 \le x \le 100$ mol% InSb (Fig. 2) is an indication for the existence of $PbSb_2Te_4$, $PbSb_2Te_4{\cdot}2InSb$, and InSb base bounded solid solutions.

The smooth course of the $d(x)$ dependence within the concentration ranges of $0 \le x \le 5$, $50.0 \le x \le 66.7$, $66.7 \le x \le 80.0$, and $95 \le x \le 100$ mol% InSb, as well as the clear maximum at x = 66.7 mol% InSb (Fig. 3) are related to the existence of the $PbSb_2Te_4{\cdot}2InSb$ compound, on the one hand, and to the existence of the bounded solid solutions based on the initial components and of the intermediate compound, on the other.

The compound $PbSb_2Te_4{\cdot}2InSb$ crystallizes in orthorhombic symmetry with unit cell parameters $a = 7.7640 \pm 0.0185$ Å; $b = 6.4144 \pm 0.0030$ Å; $c = 3.6010 \pm 0.0003$ Å; $\alpha = \beta = \gamma = 90 \pm 0.02°$. The roentgenographic data are shown in Table 2.

(c) Within the concentration ranges $10 < x < 50$ and $80 < x < 95$ the lines of two phases exist simultaneously: $PbSb_2Te_4 + PbSb_2Te_4{\cdot}2InSb$ and $PbSb_2Te_4{\cdot}2InSb$ + InSb, i.e. these concentration regions correspond to two two-phase fields in the phase diagram of the $(PbSb_2Te_4)_{1-x}(InSb)_x$ system.

The phase diagram of the $PbSb_2Te_4$–InSb system; $0 \le x \le 100$ (Fig. 4) is plotted on the basis of the XRD, DTA, and microhardness and density measuring results. It is a polythermal cross section of the three-component PbTe–Sb_2Te_3–InSb system and is characterized by the following features:

1. There are three non-variant equilibria: syntectic equilibrium with coordinates: x = 66.7 mol% InSb and $T = 530 \pm 5$ °C, and two eutectic equilibriums with coordinates: x = 90 mol% InSb and $T = 460 \pm 5$ °C, and x = 40 mol% InSb and $T = 500 \pm 5$ °C, respectively; the latter should be considered as a quasi-eutectic equilibrium.
2. As a result of the syntectic reaction

$$L_1 + L_2 \overset{530 \pm 5\,^{\circ}C}{\longleftrightarrow} PbSb_2Te_4 \cdot 2InSb(A)$$

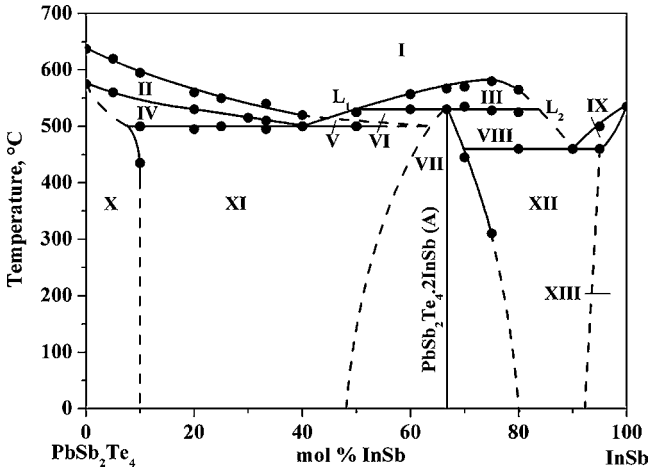

Fig. 4. Phase diagram of the $PbSb_2Te_4$–InSb system (I, L; II, PbTe + L; III, $L_1 + L_2$; IV, α-$PbSb_2Te_4$ + PbTe; V, PbTe + L + α-$PbSb_2Te_4$; VI, L + A; VII, A; VIII, A + L_2; IX, L_2 + α-InSb; X, α-$PbSb_2Te_4$; XI, α-$PbSb_2Te_4$ + A; XII, A + α-InSb; XIII, α-InSb, wherein A = $PbSb_2Te_4 \cdot (2 \pm \delta)$InSb).

an intermediate compound is formed with an asymmetric area of homogeneity shifted to the InSb-rich side ($+\delta = 0$–2), incongruently melting at 530 ± 5 °C (L_1 – liquid, rich of $PbSb_2Te_4$; L_2 – liquid, rich of InSb). The existence of the $PbSb_2Te_4 \cdot (2 \pm \delta)$InSb compound, wherein $-\delta = 0$–1 and $+\delta = 0$–2 (at room temperature), was proved by DTA and XRD, and by HV and *d* measurements. With the temperature increase the homogeneity area narrows and disappears at the melting temperature, i.e. the intermediate compound composition is $PbSb_2Te_4 \cdot 2$InSb at this temperature. The zone of limited solubility of the components $PbSb_2Te_4$ and InSb in a liquid state is located between the synthetic horizontal line and the binodal curve. The binodal curve critical point does not coincide with the composition of the intermediate compound $PbSb_2Te_4 \cdot 2$InSb as it is in most of the cases.

3. A shift of the diffraction patterns is observed at room temperature with both $PbSb_2Te_4$ (within the range from 0 to 10 mol% InSb) and InSb (within the range from 95 to 100 mol% InSb), i.e. the $PbSb_2Te_4$ dissolves up to 10 mol% InSb at this temperature, and the InSb–up to 5 mol% $PbSb_2Te_4$. When the temperature increases this solubility decreases to 0 mol% for both compounds.
4. The $PbSb_2Te_4 \cdot 2$InSb compound melts incongruently by the following reaction:

$$PbSb_2Te_4 \cdot 2InSb \overset{570 \pm 5\,^{\circ}C}{\longleftrightarrow} PbTe + L$$

This typical feature of $PbSb_2Te_4 \cdot 2$InSb is the reason for the occurrence of the three-phase area V where three phases (PbTe + $PbSb_2Te_4 \cdot 2$InSb + L) are in equilibrium and the eutectic equilibrium transformes into a quasi-eutectic equilibrium (besides liquid phase L, there was also a solid phase PbTe):

$$PbSb_2Te_4 + PbSb_2Te_4 \cdot 2InSb \overset{500 \pm 5\,^{\circ}C}{\longleftrightarrow} PbTe + L$$

The three-phase area V is surrounded by three two-phase areas: area II (PbTe + L), area VI ($PbSb_2Te_4 \cdot 2$InSb + L), and area XI ($PbSb_2Te_4 + PbSb_2Te_4 \cdot 2$InSb). The existence of area II is related to the incongruent melting of the initial $PbSb_2Te_4$ compound and therefore two temperatures exist on the ordinate at $x = 0$: $T = 575$ °C (peritectic decomposition temperature), and $T = 637$ °C (complete melting temperature).

As a result of the complex physicochemical interactions in the solid and liquid condition, an intermediate phase is formed with a composition $PbSb_2Te_4 \cdot (2 \pm \delta)$InSb, which, together with the initial components $PbSb_2Te_4$ and InSb, determine the existence of 13 phase fields, four of which are single-phase (I, VII, X, and XIII), one is three-phase (V), and the rest are two-phase fields.

4. Conclusion

1. The phase diagram of the $PbSb_2Te_4$–InSb system was plotted using four independent methods; it represents a polythermal cross section of the three-component PbTe–Sb_2Te_3–InSb system. It is characterized by the existence of an intermediate incongruently melting compound, three non-variant equilibria (syntectic, eutectic and quasi-eutectic), $PbSb_2Te_4$- and InSb-base boundary solid solutions, and thirteen phase fields (four single-phase, eight two-phase and a three-phase).
2. The compound $PbSb_2Te_4 \cdot 2$InSb is formed by a syntectic reaction. It melts incongruently at 530 ± 5 °C and has an asymmetric homogeneity area shifted to the side rich in InSb ($+\delta = 0$–2). The compound $PbSb_2Te \cdot 2$InSb crystallizes in orthorhombic symmetry with unit cell parameters $a = 7.7640$ Å; $b = 6.4144$ Å; $c = 3.6010$ Å; $\alpha = \beta = \gamma = 90^{\circ}$.
3. The $PbSb_2Te_4$ and InSb base boundary solid solutions are extended (at room temperature) from 0 to 10, and from 95 to 100 mol% InSb, respectively. Upon increase of temperature the InSb solubility in $PbSb_2Te_4$ and the $PbSb_2Te_4$ solubility in InSb smoothly decrease to 0 mol% for both compounds.

References

[1] N. Abrikosov, E. Elagina, M. Popova, Izv. AN SSSR, Neorg. Mater. 1 (1965) 2151 (in Russian).
[2] T. Hirai, Y. Takeda, K. Kurota, J. Less-Common Met. 13 (1967) 352.
[3] R. Reynolds, J. Electrochem. Soc. 114 (1967) 526.
[4] L. Shelimova, O. Karpinskii, T. Svechnikova, E. Avilov, M. Kretova, V. Zemskov, Inorg. Mater. 40 (2004) 1264.
[5] L. Shelimova, T. Sveshnikova, P. Konstantinov, O. Karpinskii, E. Avilov, M. Kretova, V. Zemskov, Inorg. Mater. 43 (2007) 125.
[6] L. Shelimova, T. Svechnikova, P. Konstantinov, O. Karpinskii, E. Avilov, M. Kretova, V. Zemskov, Proc. 5th Eur. Conf. on Thermoelectrics, Odessa, 2007, p. 10.
[7] L. Shelimova, T. Svechnikova, P. Konstantinov, O. Karpinskii, E. Avilov, M. Kretova, V. Zemskov, Proc. 2nd Eur. Conf. on Thermoelectrics, Krakow, 2004, p. 202.
[8] M. Hansen, K. Anderko, Constitution of Binary Alloys, McGraw-Hill Book Co., NY, 1958.
[9] Joint Committee on Powder Diffraction Standards, Powder Diffraction File 06-0208.
[10] J. Wooley, P. Keating, J. Less Common Met. 3 (1961) 194.
[11] C. Kittel (Ed.), Introduction to Solid State Physics, 6th Edition, John Wiley, NY, 1986, p. 185.
[12] T. Ito, X-ray Studies on Polymorphism, Maruzen Co. Ltd., Tokyo, 1950, p. 187.